Supporting Information

A Silicon Anode for Garnet-Based All-Solid-State Batteries: Interfaces and Nanomechanics

Weiwei Ping,[1a] Chunpeng Yang,[1a] Yinhua Bao,[2a] Chengwei Wang,[1] Hua Xie,[1] Emily Hitz,[1] Jian Cheng,[2] Teng Li,[2*] Liangbing Hu[1*]

[1]Department of Materials Science and Engineering, University of Maryland, College Park, Maryland, 20742
[2]Department of Mechanical Engineering, University of Maryland, College Park, Maryland, 20742
[a] W.P., C.Y., and Y.B. contributed equally
[1*] Email: binghu@umd.edu
[2*] Email: lit@umd.edu

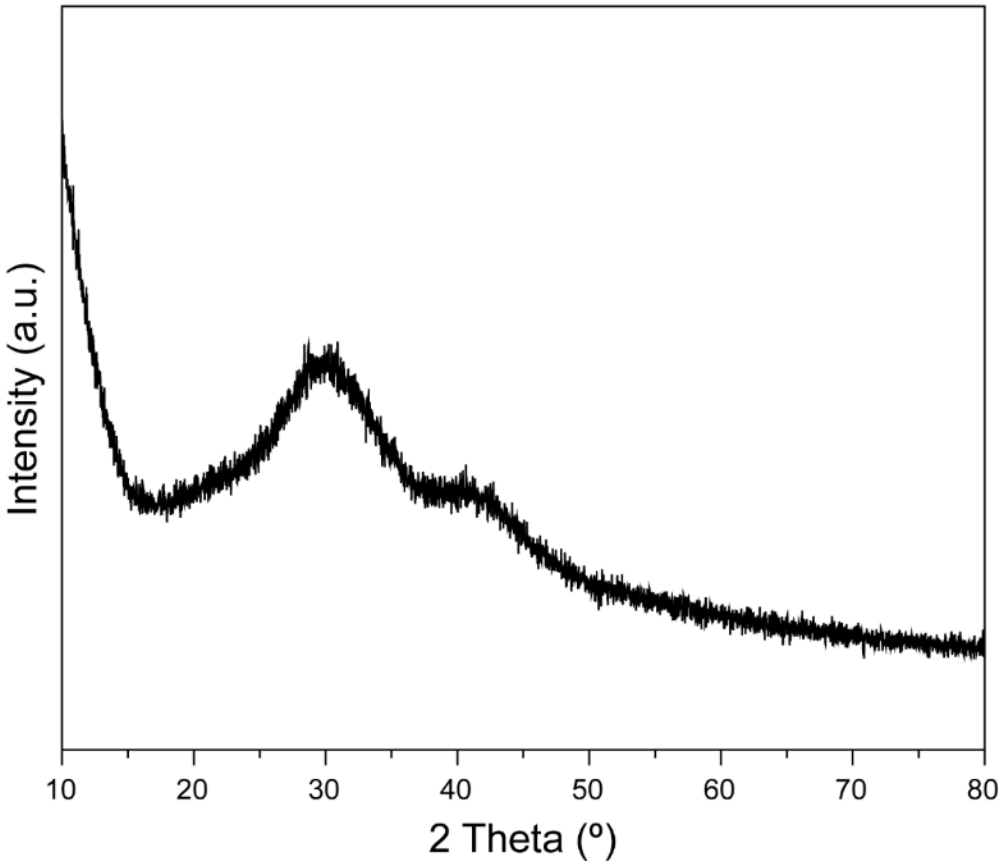

Figure S1. XRD characterization of 1 μm Si film deposited on an amorphous substrate. The XRD profile shows that the Si film deposited by PECVD is amorphous.

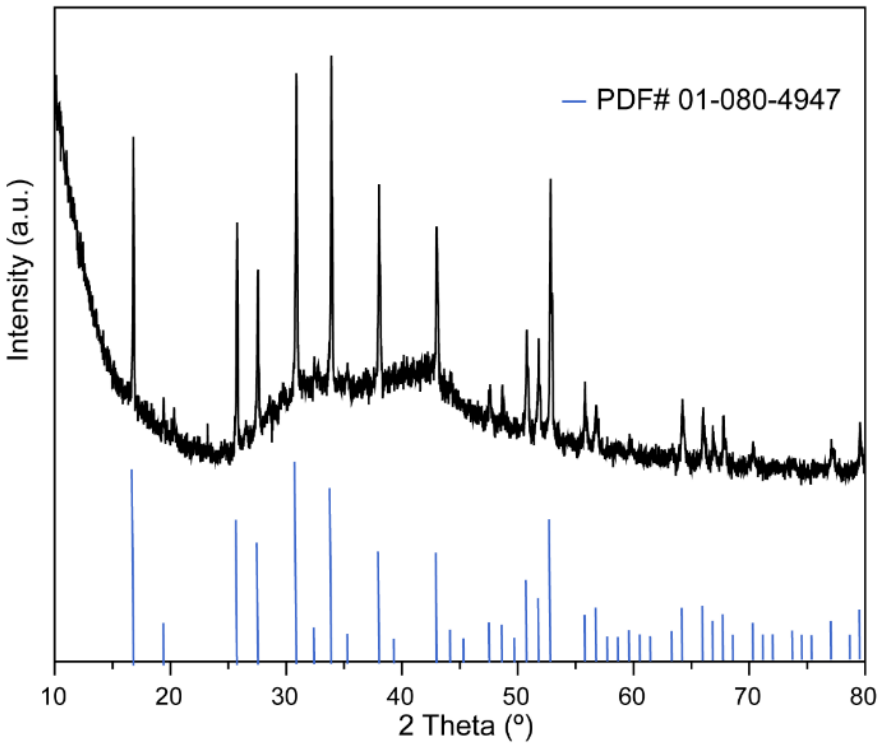

Figure S2. XRD of garnet ($Li_7La_3Zr_2O_{12}$). The XRD shows that the garnet Al-doped $Li_7La_3Zr_2O_{12}$ exhibit the cubic crystal structure without other second phase.

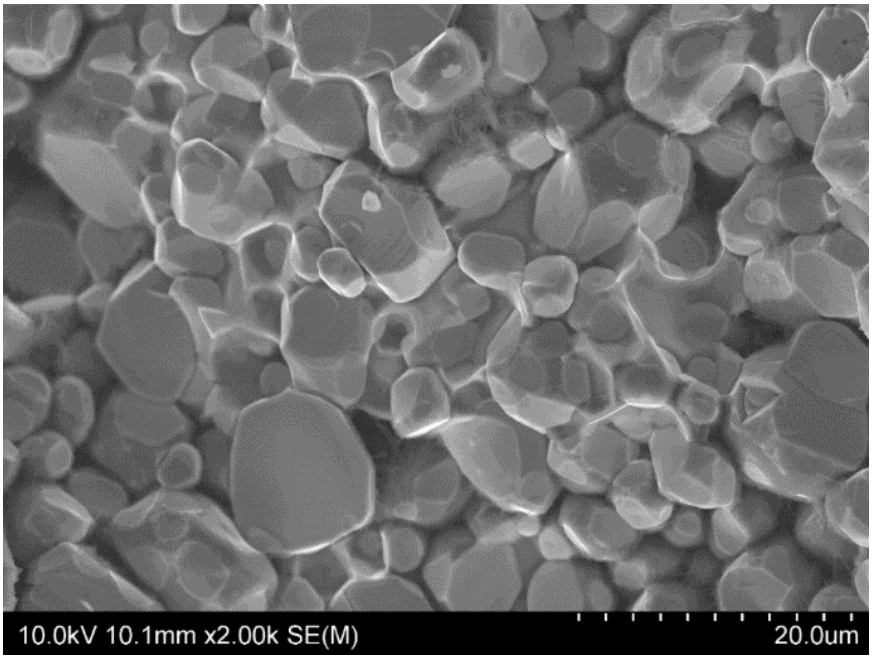

Figure S3. SEM of garnet ($Li_7La_3Zr_2O_{12}$). The garnet grains are uniformly distributed and in tight contact with each with low porosity.

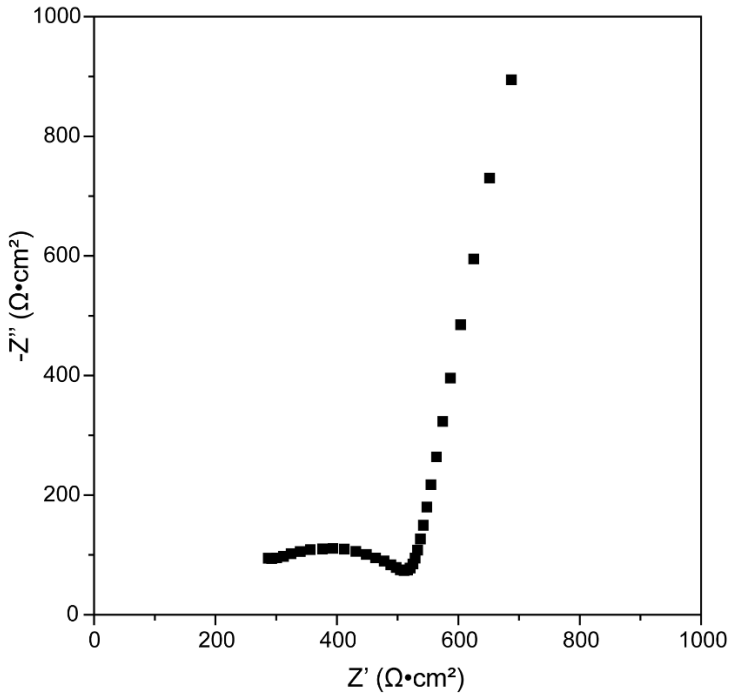

Figure S4. Impedance spectrum of garnet ($Li_7La_3Zr_2O_{12}$). The impedance of garnet is low, exhibiting a high ionic conductivity of 4 $\times 10^{-4}$ S/cm.

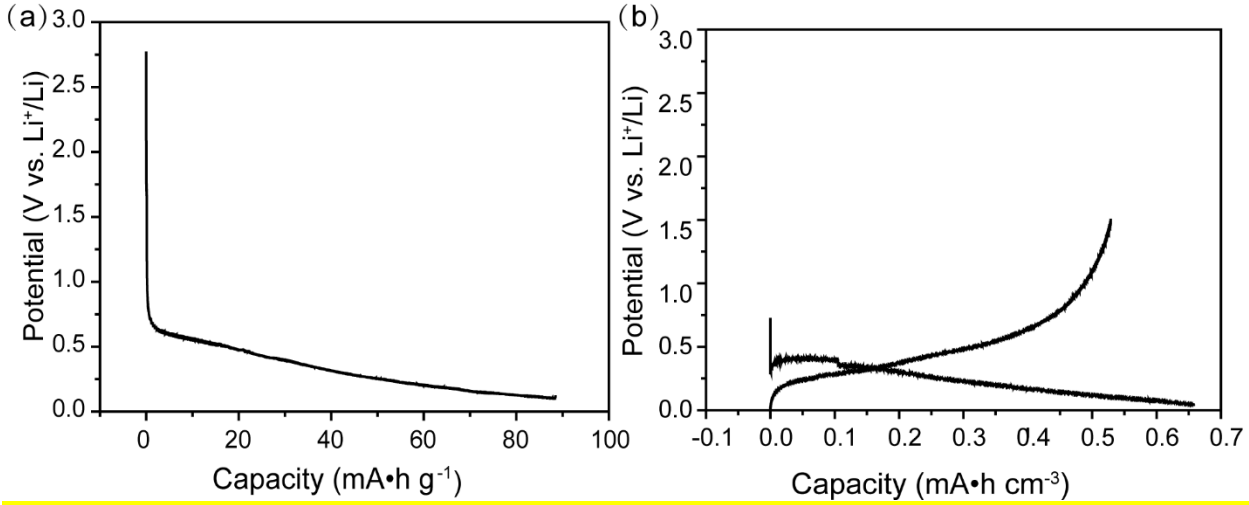

Figure S5. (a) Electrochemical performance of the CNT anode. (b) Voltage profile of the Si anode in the solid-state battery.

The cell Li/garnet/Si contributed an irreversible capacity of ~ 90 mA h g^{-1}. The discharge areal capacity of the 1 μm Si anode was ~ 0.66 mA h cm^{-2}. The charge areal capacity of the 1 μm Si anode was ~ 0.53 mA h cm^{-2}.

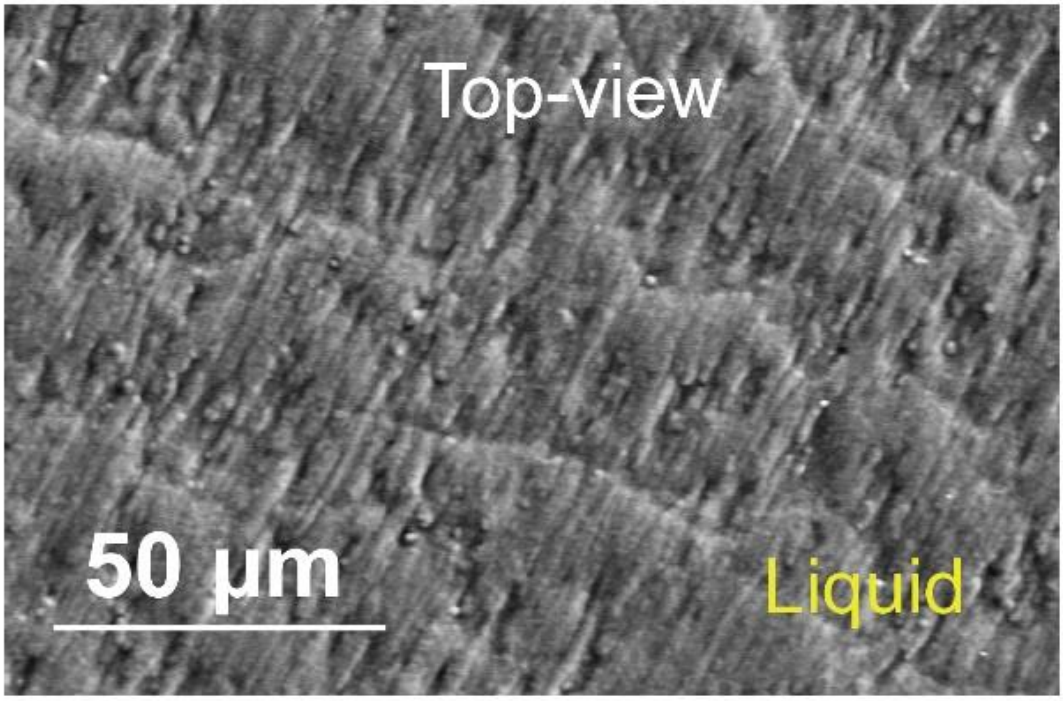

Figure S6. Morphology of the 1 μm Si anode on Cu foil.

The Si anode appears dense and uniformly deposited on Cu foil by PECVD.

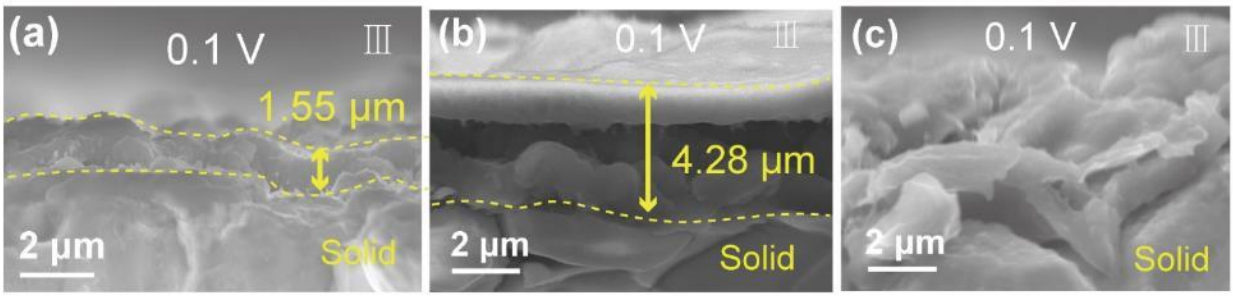

Figure S7. Cross-sectional SEM images of (a) 1 μm, (b) 2 μm and (c) 3 μm Si anodes discharged to 0.1 V.

The 1 μm Si anode remains tight contact with the garnet electrolyte after discharging to 0.1 V. Even though there was no obvious crack between the 2 μm Si anode and garnet interface, the 2 μm Si anode began to show some damage inside. In comparison, the 3 μm Si anode separated from the garnet after discharging to 0.1 V.

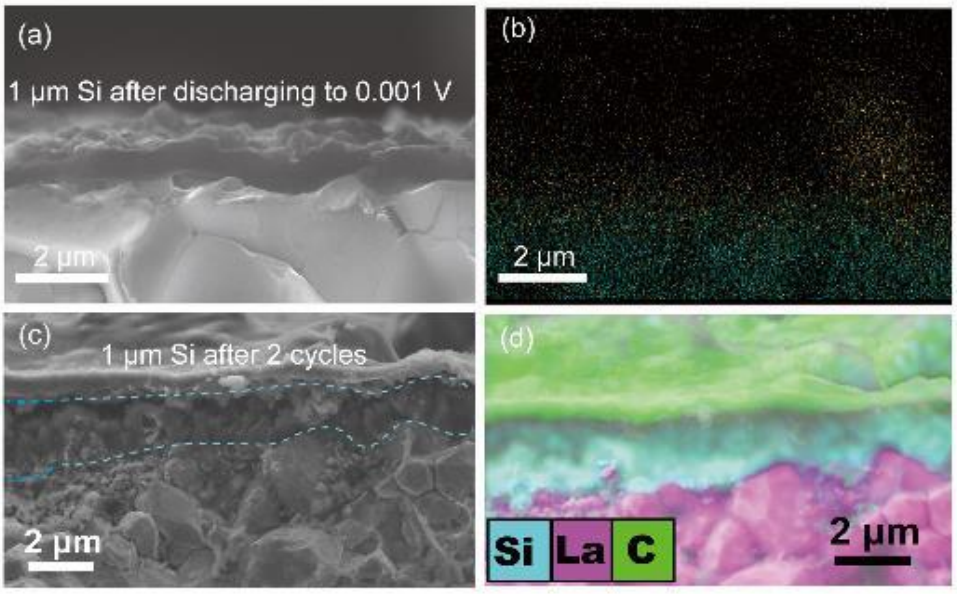

Figure S8. Magnified cross-sectional SEM of (a) 1 μm Si anode discharging to 0.001 V, (b, d) mapping images, and (c) after 2 discharge/charge cycles.

The 1 μm Si anode maintains good contact with the garnet after discharging to 0.001 V and even after two discharge/charge cycles.

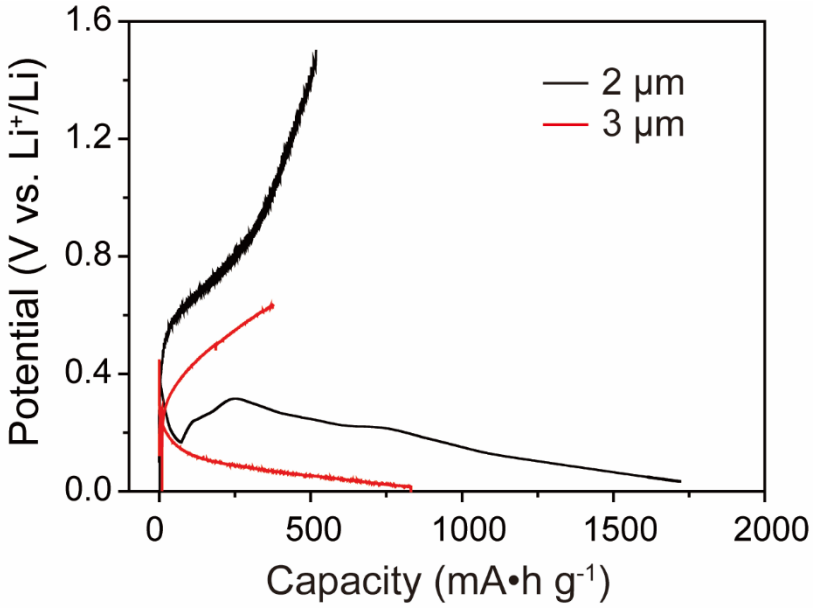

Figure S9. Voltage profile of the 2 μm and 3 μm Si anodes in the solid-state battery configuration. The Li/garnet/Si cell featuring the 2 μm Si anode exhibited a discharge capacity of 1713.8 mA h g^{-1}, much higher than that of the 3 μm Si anode, which was 831.7 mA h g^{-1}.

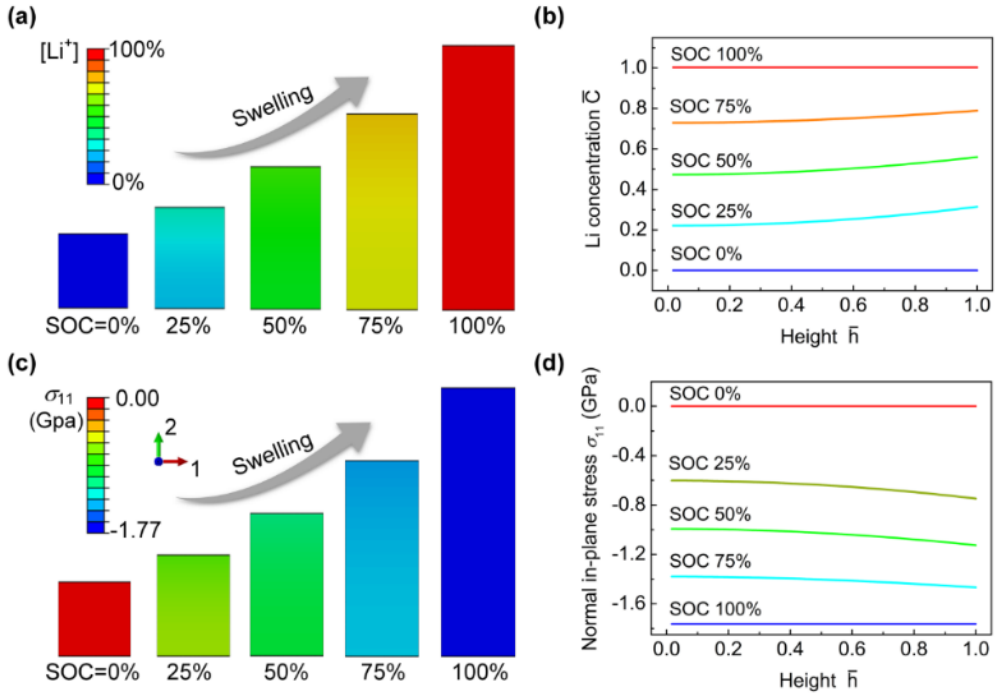

Figure S10. The Li concentration and stress distribution of the Si anode under lithiation in the solid-state battery. Snapshots of the distribution of the (a) normalized Li ion concentration and (c) in-plane stress component of the Si anode during lithiation. (b) The Li ion concentration and (d) in-plane stress component versus the location along the film thickness. The discharge rate in the simulation was 0.0188 C.

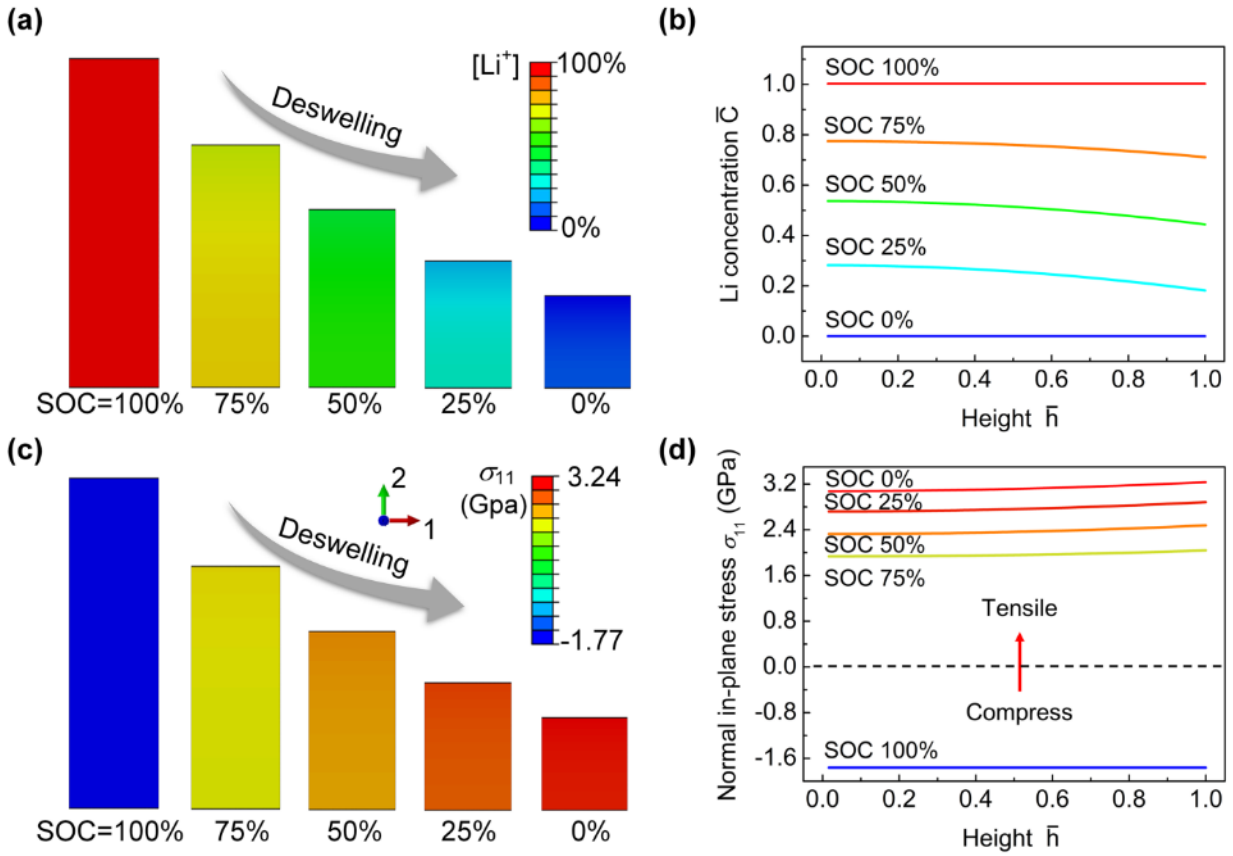

Figure S11. The Li concentration and stress distribution of the Si anode under delithiation in the solid-state battery. Snapshots of the distribution of (a) normalized Li ion concentration and (c) in-plane stress component of the Si anode during delithiation. (b) The Li ion concentration and (d) in-plane stress component versus location along the film thickness. The charge rate in the simulation was 0.0188 C.

Based on our simulation, the thickness of the Si anode increases/decreases by approximately 3 folds during lithiation and delithiation, respectively, which is in accordance with the experimental observations. The Li concentration and stress distribution are uniform in both the lithiation and delithiation state due to the slow charge rate.

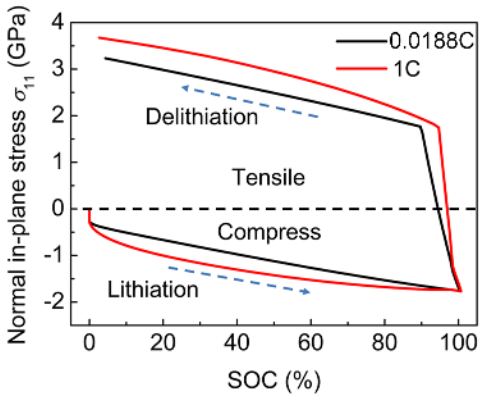

Figure S12. The normal in-plane stress distribution at the surface of the Si anode during lithiation and delithiation under slow (black) and fast (red) charge rates of 0.0188 C and 1 C, respectively.

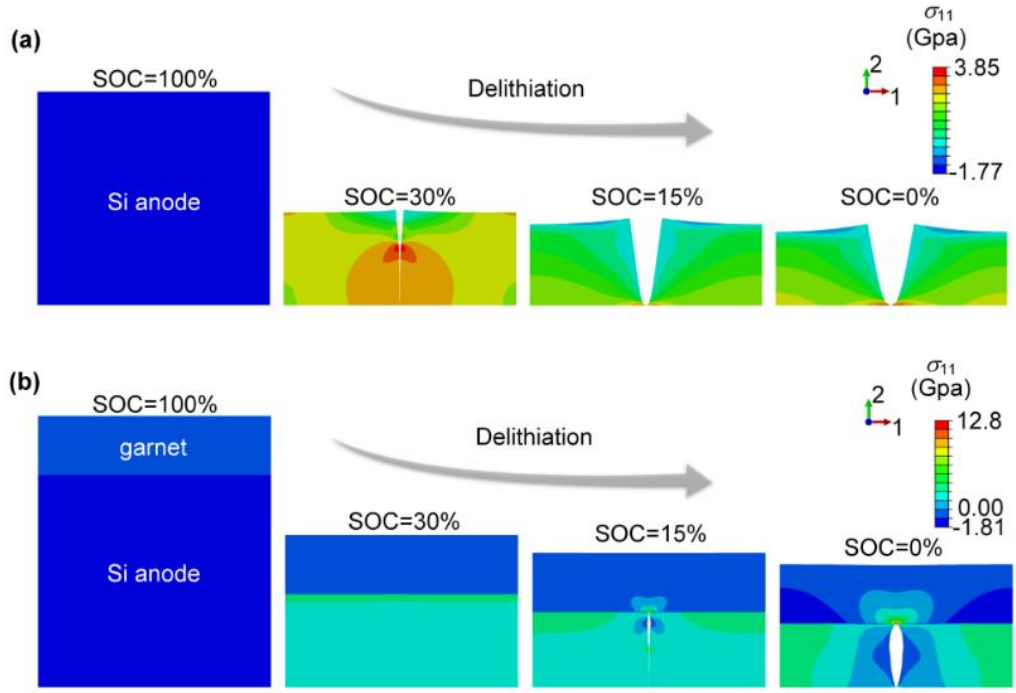

Figure S13. The morphology evolution of the defective part in the Si anode (a) without garnet and (b) with garnet during delithiation. The color contours denote the in-plane stress (σ_{11}) level.

At different SOC (30%, 15%, 0%), the crack opening displacement in the Si anode with garnet electrolyte is much smaller than the displacement in the Si anode without garnet, showing the

robust mechanical constraint provided by the solid garnet to maintain the battery's structural integrity.

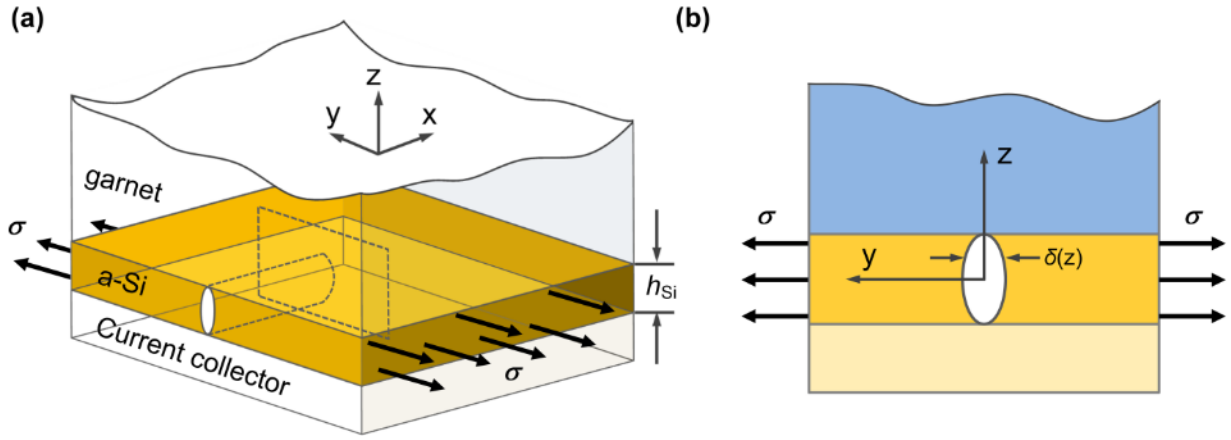

Figure S14. (a) Theoretical model of the steady advance of a tunnel crack in Si anode embedded between garnet-type solid electrolyte and the current collector at the delithiation state. (b) The y-z cross-section at the tunnel crack front; $\delta(z)$ is the crack opening profile for the plane strain through-crack.

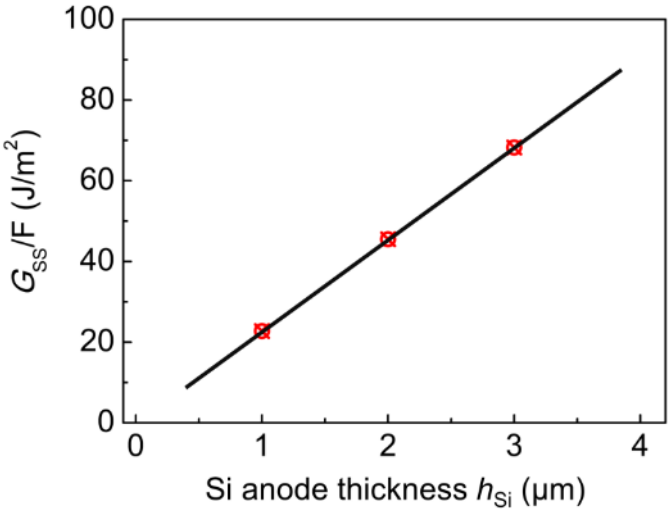

Figure S15. The linear relation between the steady-state energy release rate G_{SS} and Si anode thickness h_{Si}. F is a dimensionless function of the moduli ratios and thickness ratios of garnet and current collector layers, which is a constant for a given structure of the garnet and current collector layers in solid state battery.

The thicker Si anode provides much higher energy release rate, making the defective part of the Si anode much easier to crack during delithiation.

Table S1. Parameters used in mechanics modeling

Parameters	Values
$E_{Si}(c)$, Young's Modulus of a-Si	130-40 GPa
$E_{Sip,}$ Plastic modulus of a-Si	1.8 GPa
Poisson ratio	0.3
$\varepsilon_{Y,}$ yielding strain of a-Si	0.2%
E_{LLZO}, Young's Modulus of LLZO[1]	147 GPa
C_{max} Maximum Li concentration	3.667e-7 mol m^{-3}
D_0, Diffusivity	10^{-14} m s^{-1}
$R,$ Gas constant	8.314 $JK^{-1}mol^{-1}$
T, Room Temperature	300K
$\beta,$ Expansion coefficient	0.44

Detailed finite element modeling (FEM) method

To understand the Li ion concentration and stress distribution of the Si anode in solid-state battery, we modeled the lithiation/delithiation (discharging/charging) process and corresponding mechanical state of the Si anode through a fully coupled diffusion-displacement analysis using the commercial finite element code ABAQUS 6.13. The model was considered at the plain strain condition. The thickness of the Si film and current collector was 1 μm, respectively. The electrochemical and mechanical parameters used in the simulation are given in Table S1. For capturing the single-phase reaction property in the amorphous Si anode, the concentration-dependent diffusivity was set in the model as $D=D_0(1+c/(1-c))$, in which D_0 is a diffusivity constant, and c is the normalized Li ion concentration. The nominal constant Li flux J (0.0188 C) is given at the top surface of the Si anode, according to the experimental galvanostatic result. The state of charge (SOC) is defined as the current lithiation capacity divided by the maximum

lithiation capacity observed in the experiment. SOC ranges from 0 to 1 during charge/discharge cycles. The Si anode was assumed to be a bilinear elastic-plastic material. The elastic module is linearly Li ion concentration dependent, which changed from 130 GPa (a-Si, c=0) to 40 GPa (lithiated a-Si, c=1). For modeling the defective part of the amorphous Si anode, cohesive zone elements were implemented straight along the direction of the Si anode thickness to model the most probable penetrate crack in the Si anode. The toughness of the lithiated a-Si and cohesion strength[2] were set to 15 J/m^2 and 2.5 GPa. Viscosity stabilization of the cohesive zone elements was employed to improve FEM numerical convergence. The garnet/a-Si interface is also simulated by a cohesive zone model, in which the interfacial toughness of the garnet/a-Si interface was assumed to be 20 J/m^2 to ensure the strong bonding between them.

Impact of the amorphous Si anode thickness on the electrochemical performance degradation

To qualitatively understand the impact of the different Si thicknesses on the degradation of the anode's electrochemical performance, we simplified the anode as a linear elastic material during delithiation. The mechanistic understanding of the failure behaviors in the Si anode during delithiation is still valid. As shown in Figure S14a, due to the constraint of the current collector and garnet, the tunnel crack at the Si anode is considered as the major failure mode during discharging/charging. A tensile stress σ exists in the Si anode during delithiation process, which is nearly a constant along the Si anode thickness according to the modeling results in Figure S11d.

In steady-state, the energy releases for an entire tunnel front advancing a unit equals to strain energy difference between the slice of unit thickness far ahead of the front and far behind of the front[3]. Meanwhile, this strain energy difference ΔU equals the work done by the stress through the crack opening (Figure S14b), which is given by,

$$\Delta U = \frac{1}{2}\sigma \int_{-h_{\mathrm{Si}}/2}^{h_{\mathrm{Si}}/2} \delta(z)\, dz \tag{1}$$

in which σ is the uniform tensile stress on the prospective crack plane prior to cracking; h_{Si} is the thickness of the Si anode, δ(z) is the crack opening profile for the plane strain through-crack.

On the other hand, the steady-state energy release rate for the through-crack is,

$$G_{SS} = \Delta U / h_{\mathrm{Si}} \tag{2}$$

Combining the Equation 1 and 2 gives,

$$G_{SS} = \frac{1}{2h_{\mathrm{Si}}}\sigma \int_{-h_{\mathrm{Si}}/2}^{h_{\mathrm{Si}}/2} \delta(z)\, dz \tag{3}$$

In steady-state tunnel crack, the above equation can be integrated as follows[4],

$$G_{SS} = \frac{1-\nu_{\mathrm{Si}}^{\,2}}{E_{\mathrm{Si}}}\sigma^2 h_{\mathrm{Si}} F\ , \tag{4}$$

where ν_{Si}, E_{Si}, and h_{Si} are the Poisson ratio, Young's Modulus and thickness of the Si anode, respectively; σ is the uniform tensile stress in Si anode; F is a dimensionless function of the moduli ratios and thickness ratios of garnet and current collector layers. It should be noted that F is a constant for a given structure of garnet and current collector layers in solid state battery. Consequently, the steady-state energy release rate has a linear correlation with the thickness of Si anode.

Experiments have suggested that the lithiated a-Si anode yields[5] at around ~ 1 GPa, when the lithiated a-Si anode has Young's Modulus E_{Si} ~ 40 GPa, Poisson ratio ν_{Si} ~ 0.3. The relation between steady-state energy release rate and the thickness of Si anode is quantitatively shown in Figure S15. The steady-state energy release rate increases linearly as the Si anode becomes thicker from 1 μm to 3 μm, which means thicker anodes crack more easily during the delithiation stage, causing the electrochemical performance to degrade.

Reference:

[1] X. Wang, S. S. Singh, T. Ma, C. Lv, N. Chawla, H. Jiang, *Chem Mater* **2017**, *29*, 5831-5840.

[2] S. M. Khosrownejad, W. A. Curtin, *J Mech Phys Solids* **2017**, *107*, 542-559.

[3] L. B. Freund, S. Suresh, *Cambridge University Press*, **2004**; 238-240

[4] V. A. Sethuraman, M. J. Chon, M. Shimshak, V Srinivasan, P. R. Guduru, *J Power Sources.* **2010,** 195, 5062-5066.

[5] Y. An, H. Jiang, *Model Simul Mater Sci*. **2013**, 21, 074007.